Zeitschrift für Physikalische Chemie, Bd. 202, S. 31–43 (1997)


# Adsorption and Reaction of Ethene on $Cr_2O_3(0001)/Cr(110)$

By I. Hemmerich, F. Rohr, O. Seiferth, B. Dillmann and H.-J. Freund*

Lehrstuhl für Physikalische Chemie I, Ruhr-Universität Bochum, 44780 Bochum, Germany
* Fritz-Haber-Institut der Max-Planck-Gesellschaft, 14195 Berlin-Dahlem, Faradayweg 4–6, Germany

(Received June 4, 1996)

*Chromium oxide / Ethene / Polymerization*

Adsorption of Ethene on a clean and oxygen precovered $Cr_2O_3(0001)$ film, grown on a Cr(110) surface, is studied via thermal desorption spectroscopy (TDS), infrared reflection absorption spectroscopy (IRAS), electron energy loss spectroscopy (EELS) and X-ray photoelectron spectroscopy (XPS). On the clean $Cr_2O_3(0001)$ surface a weakly chemisorbed and a physisorbed state of ethene may be identified via TDS, IRAS and electron spectroscopies. Under ultrahigh vacuum conditions adsorption and desorption of ethene is fully reversible for both, the clean and the oxygen precovered chromiumoxide surface with peak maxima below room temperature. If the sample, however, is heated to above room temperature under a background pressure of ethene, the formation of hydrocarbons on the surface is observed which may be only removed from the surface by applying higher temperatures coupled with sputter anneal treatments. We interpret these findings as the consequence of a polymerization reaction of ethene on the oxide surface. Polymerization is discussed in the context of the mechanism of low pressure polymerization with the Phillips process.

Die Adsorption von Ethen auf einem reinen und einem Sauerstoff-vorbelegten $Cr_2O_3(0001)$-Film, aufgewachsen auf einer Cr(110)-Oberfläche, wird mittels Thermischer Desorptionsspektroskopie (TDS), Infrarot-Reflexions-Absorptionsspektroskopie (IRAS), Elektronen-Energieverlustspektroskopie (EELS) und Röntgenphotoelektronenspektroskopie (XPS) untersucht. Auf der reinen $Cr_2O_3(0001)$-Oberfläche können ein schwach chemisorbierter und ein physisorbierter Zustand von Ethen über TDS, IRAS und Elektronenspektroskopien nachgewiesen werden. Im Ultrahochvakuum sind Adsorption and Desorption des Ethens sowohl für die reine als auch für die Sauerstoff-vorbelegte Chromoxidoberfläche voll reversibel, wobei die Desorptionstemperaturen unterhalb von Raumtemperatur liegen. Wird die Probe allerdings oberhalb von Raumtemperatur und unter einem Hintergrundgasdruck von Ethen geheizt, kann die Bildung von Kohlenwasserstoffen beobachtet werden, die nur bei Anwendung hoher Temperaturen verbunden mit Sputtern wieder von der Oberfläche entfernt werden können. Wir deuten diese Beobachtungen als Ergebnis einer Polymerisationsreaktion von Ethen auf der Oxidoberfläche. Diese Polymerisation wird in Bezug auf den Mechanismus Niederdruckpolymerisation im Phillips-Prozeß diskutiert.

## 1. Introduction

In previous studies several groups have reported on the pronounced reactivity of $Cr_2O_3$ surfaces [1–14]. These studies include investigations on polycrystalline as well as on single crystalline surfaces. Recently, Zecchina and his group [5] have presented infrared data on the interaction and polymerization of ethene on microcrystalline chromiumoxide surfaces. They point out that their results may have implications for a microscopic understanding of the mechanism of the Phillips process for which various proposals for the active site have been made in the past [1, 4, 15, 16]. However, a generally accepted view on the mechanism has not been presented so far. Briefly, the catalyst in this case consists of chromia deposited on a silica support. There are some early indications, in particular from the work of McDaniel and coworkers [2, 16] and J. Lunsford's group [17] that the relevant chromium species activating the ethene molecule may be either a $Cr^{2+}$ species or a coordinatively unsaturated $Cr^{3+}$ species. I. Wachs *et al.* [18, 19] have recently published reviews collecting infrared data of supported chromia model catalysts. From these data the presence of Cr–O-bonds on the surface of the catalysts and their influence on reactions have been deduced. It will be very interesting in the future to compare the data gained on the polycrystalline material with those on thin oxide films, which may be investigated via FTIR techniques (see for example [20]).

In general, there is a need for surface science based studies on relevant adsorption systems in which well defined oxide surfaces of a given crystallographic orientation are employed. In the present study we report a combined TDS, IRAS, EELS and XPS-study of the adsorption behaviour of ethene on a clean and oxygen modified $Cr_2O_3$(0001) surface. We identify several adsorption states depending on the pretreatment of the surface. Indications are found that the clean $Cr_2O_3$(0001) surface induces polymerization at slightly elevated temperatures and higher pressures (in the 1 bar regime), while the oxygen precovered surface is inactive.

## 2. Experimental

The experiments have been performed in several ultrahigh vacuum systems.

For the XPS measurements a double chamber system has been used. One chamber, layed out as a preparation unit was used for preparation of the oxide surface via oxidation of a Cr(110) single crystal surface applying well know recipes [8–11]. Surface order was checked via electron energy diffraction (LEED) with particular emphasis of the observability of the surface phase transition which has been noted as a good indicator for the cleanliness of the surface [12]. In the same chamber the surface was dosed

with ethene. A separate compartment in the preparation chamber even allowed an exposure to higher (1 bar regime) pressures. Pressure control was limited. The analysis chamber allowed for non-monochromatized and monochromatized XPS measurements. For data accumulation the readout of the employed LHS 11 analyser has been substantially modified [21], so as to allow for parallel detection of 18 channels and storage of the information within 1 μ sec including dead time for reset.

The EELS measurements have been carried out in a second apparatus which was also consisting of a preparation and analysis unit. This analysis chamber was equipped with angle resolved photoemission and electron energy loss modules. The overall resolution of the electron energy loss spectrometer was 25 meV.

For EELS studies with higher resolution a third double-chamber system was used containing an ELS 22 unit. Here the resolution was below 10 MeV. Recently, this apparatus was extended with a Mattson RS-1 FTIR spectrometer to perform IRAS measurements in grazing incidence geometry. Details of the experimental setup are discussed elsewhere [22].

The TDS spectra included in this paper have been taken in a forth chamber. This apparatus was equipped with a quadrupole mass spectrometer and a specially designed doser system [23].

## 3. Results and discussion

Fig. 1 shows thermal desorption spectra of the ethene dosed $Cr_2O_3$(0001) surface. At very low coverage there is one desorption feature observed in the range of 230 K. We associate the peak at 230 K with adsorption at regular terrace sites. The maximum temperature decreases with increasing coverage. With increasing coverage an additional signal at lower desorption temperature (below 150 K) can be observed.

These TD-spectra should be compared with those obtained after saturating the surface with molecular oxygen at low temperature before ethene dosage (see Fig. 2). In this case the exposure to 25 L ethene with and without oxygen predosage are compared. Clearly, the main observation is the strong attenuation of the ethene signal by about one order of magnitude. However, the features in the spectrum remain although slightly shifted, in particular for the desorption feature above 200 K peak temperature. We take this as indication that the ethene is chemically interacting with the metal ions on the surface. We know from a detailed study of oxygen adsorption employing infrared reflection absorption spectroscopy that oxygen interacts strongly with the metal ions on the surface, thus blocking them to a large extent for interaction with ethene [20]. A detailed account of the interaction of oxygen with a $Cr_2O_3$(0001) surface will be given elsewhere [24].

The infrared reflection absorption spectra of the ethene adsorption on $Cr_2O_3$(0001) support the TDS-results. Fig. 3 shows a series of IRA-spectra

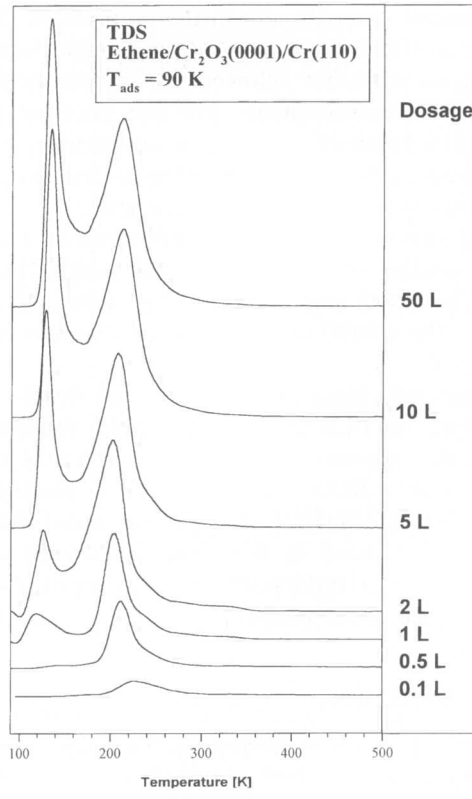


**Fig. 1.** Thermal desorption spectra of ethene from clean $Cr_2O_3$(0001) for various dosages.

recorded after the chromium oxide surface has been dosed with increasing exposures of $C_2H_4$. At very low coverages ($\leq$1 L) we can detect only one vibrational feature around 1010 $cm^{-1}$. This band can be assigned to the C−H out of plane wagging mode $\gamma_\omega(B_{3u})$ of ethene (949 $cm^{-1}$ in the gas phase [25]) which is shifted to higher frequencies upon adsorption on $Cr_2O_3$(0001). A similar behaviour (992 $cm^{-1}$ for $\gamma_\omega(B_{3u})$) was found in the IR-spectra of the adsorption of $C_2H_4$ on microcrystalline chromiumoxide [5]. The upward shift was taken as indication for the interaction of ethene with the electron-withdrawing chromium ions of the substrate [5].

As the ethene exposure to $Cr_2O_3$(0001) is increased, the band of the $\gamma_\omega$-mode becomes broader and a shoulder at around 998 $cm^{-1}$ grows up (see Fig. 3). In addition, a second vibrational feature at around 2980 $cm^{-1}$ is observed which can be attributed to the symmetric C−H stretching vibration of adsorbed $C_2H_4$. These changes in the IRA-spectra are in accordance with the appearance of the low-temperature desorption feature in the

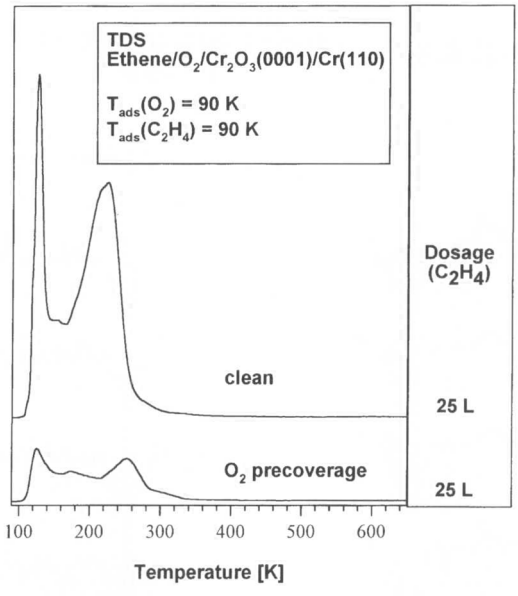


**Fig. 2.** Thermal desorption spectra of ethene from oxygen presatured $Cr_2O_3$(0001) surface.

TDS at increasing coverages. So the TDS as well as the infrared data support the distinction between physisorbed and chemisorbed ethene molecules on the $Cr_2O_3$(0001) surface.

The dipole selection rule of IRA-spectroscopy on metal samples [26] allows to determine adsorption geometries. Assuming that the rule holds also for thin oxide films grown on metal single crystals, the chemisorbed ethene molecules are adsorbed with their molecule plane more or less parallel to the $Cr_2O_3$(0001) surface. Namely, the symmetric C−H stretching vibration which lies in the molecular plane is not detectable for exposures below 1 L where all the adsorbed ethene is bound as chemisorbate. In contrast, in the physisorbed state the geometry is less well defined.

The TDS and IRAS results are corroborated by XPS measurements. Fig. 4 collects $Cr2p_{3/2}$ XP spectra of clean $Cr_2O_3$(0001) as compared with the oxygen exposed, the ethene exposed and the co-exposed surface.

The $Cr2p_{3/2}$ signal shows a fine structure as has been discussed before [10, 11, 27]. The peak at lowest binding energies has been partly associated with the surface chromium ions. It is the reduced coordination in the surface that leads to the surface chemical shifts of the chromium ionization [12]. Upon oxygen adsorption the whole feature is shifted by 0.4 eV to lower binding energy with respect to the weak metal signal at 574 eV which does not shift. Concomitantly, the surface signal at 575.8 eV is reduced (see difference spectra determined after correcting for the general shift). To under-

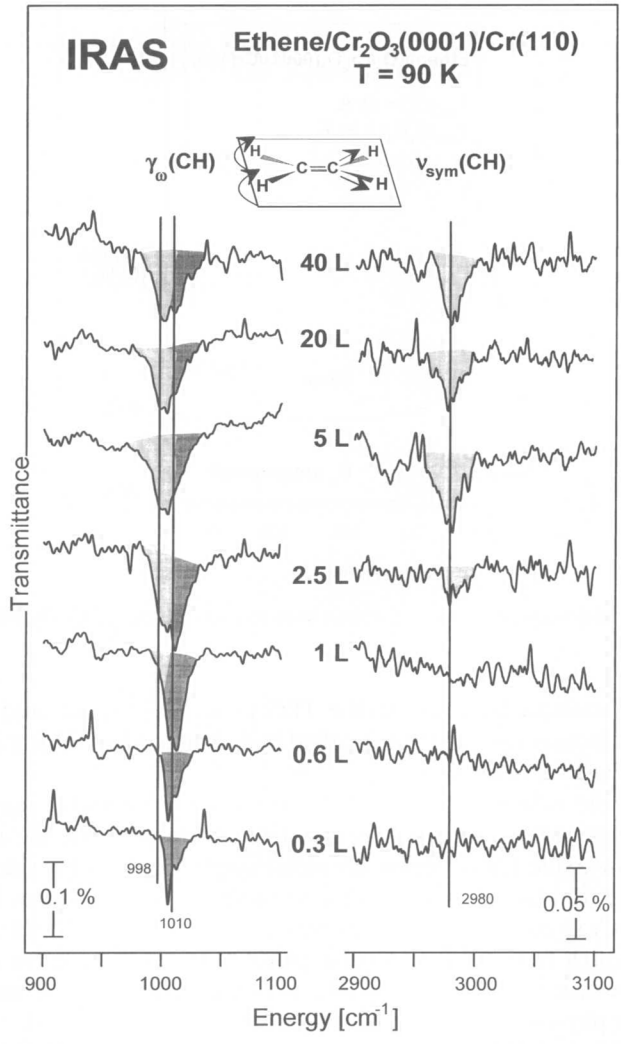


**Fig. 3.** Infrared reflection adsorption spectra of ethene on $Cr_2O_3(0001)$ surface for various dosages.

stand the shift we have to consider the system consisting of an oxide layer on top of a metal substrate. The polar oxide layer establishes a space charge region in front of the metal surface equivalent to a dipole. Any adsorption on the oxide surface will change the space charge, therefore the dipole moment and thus shift all levels of the system [28, 29]. Electron withdrawing adsorbates will shift the level to lower binding energies because the dipole is reduced. Electron donating adsorbates will shift the levels to

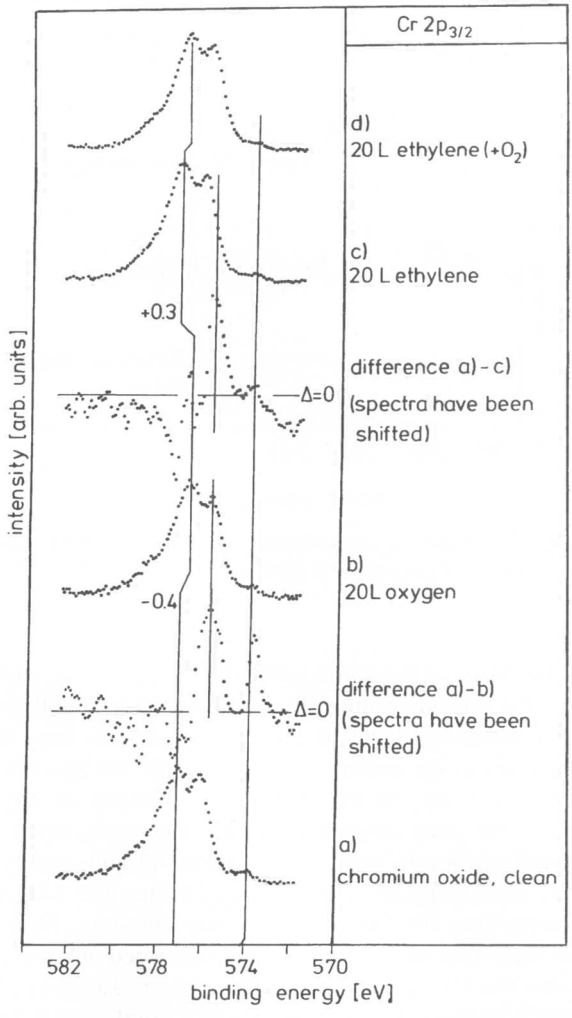


**Fig. 4.** $Cr2p_{3/2}$ photoelectron spectra of the clean, oxygen covered, ethene covered and co-exposed $Cr_2O_3$(0001) surfaces. Difference spectra between clean and adsorbate covered surfaces are included.

higher binding energies. The shift is thus interpreted as an initial state effect caused by the formation of the oxygen-chromium bonds which are polarized from the metal ions towards oxygen thus causing a lowering of the binding energy. In contrast to the situation after oxygen adsorption, ethene exposure leads to a similar decrease in the surface signal (see difference spectrum) but a shift of the $Cr2p_{3/2}$ feature as a whole by 0.3 eV to higher binding

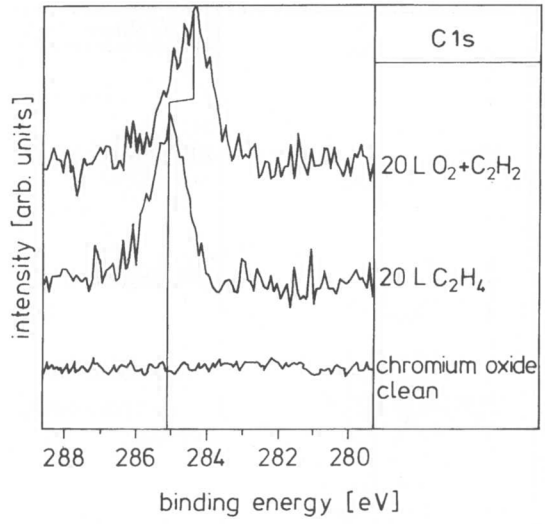


**Fig. 5.** C1s photoelectron spectra of the ethene covered $Cr_2O_3$(0001) surface compared with the ethene covered oxygen predosed surface.

energies. On the basis of the same concept this shift is an indication for a polarization at the surface from ethene towards the metal ions. In other words ethene is donating electrons onto the chromium ions. If ethene and oxygen are exposed to the surface simultaneously, we again find a shift to lower binding energy due to the preferential sticking of oxygen but not quite as large as for pure oxygen exposure. However, upon exposing an oxygen predosed surface to ethene no further binding energy shift is observed. This is interpreted as a lack of any noticeable charge-transfer or polarization interaction for the weakly interacting state. Shifts in the O1s signals of the oxide (not shown) reflect the described situation as well.

Fig. 5 shows the C1s spectra for ethene on $Cr_2O_3$(0001) and compares the pure ethene adsorbate with the oxygen predosed adsorbate. Due to the very weak coupling of ethene to the oxygen precovered surface, the C1s ionization basically follows the shift of the substrate ionizations to lower binding energies. The binding energy of 284.9 eV for the pure ethene adsorbate is compatible with binding energies observed for unsaturated hydrocarbons on metal [30–32] and oxide [33, 34] surfaces.

Electron energy loss spectra taken in the electronic regime clearly indicate the interaction of ethene with the metal ions. Fig. 6 shows the spectrum of the clean surface with the typical excitations of the surface chromium ions. Those have been discussed and assigned in detail elsewhere [8, 12]. Upon adsorption of ethene the surface excitations are strongly attenuated (see Fig. 6) and the transitions on the ions in the bulk environment remain.

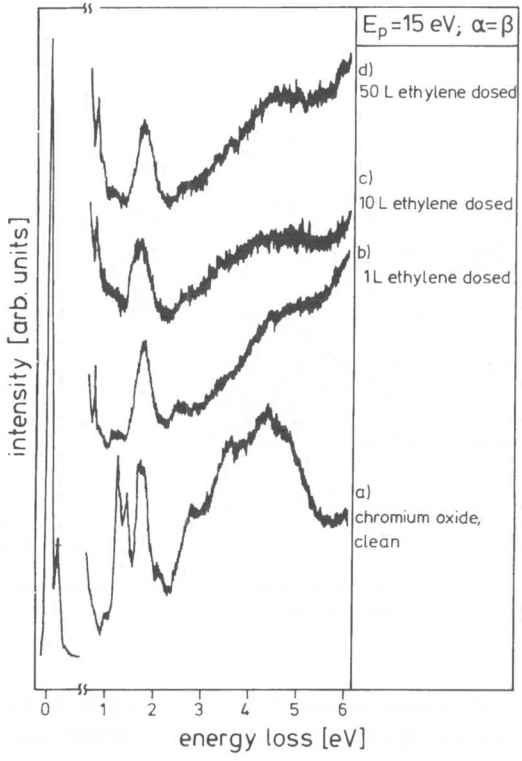


**Fig. 6.** ELS-spectra in the electronic regime of the clean and ethene exposed surface.

The sharp transition at 750 meV corresponds most probably to a double excitation of the C−H stretching vibrations. It is also conceivable that this excitation is due to chromium ions which have changed their oxidation state [21], but this is unlikely as we shall discuss below. Summarizing at this point, we find that ethene chemisorbs onto the metal ions in the first layer of chromium oxide, probably via a small charge-transfer of electrons into the oxide surface. We note that adsorption under ultrahigh vacuum conditions is fully reversible, i.e. upon heating the surface ethene desorbs without any noticeable residue.

The situation changes if the surface is heated in an ethene atmosphere. It is important to realize that the oxide surface was not predosed with oxygen prior to this treatment. Fig. 7 and Fig. 8 contain the relevant XPS and EELS data. After the above treatment the surface is covered with a hydrocarbon layer which cannot be removed by simply heating the surface. Its carbon 1s spectrum (Fig. 7 right hand side) indicates that even after heating to 520 K when all chemisorbed ethene under ultrahigh vacuum conditions

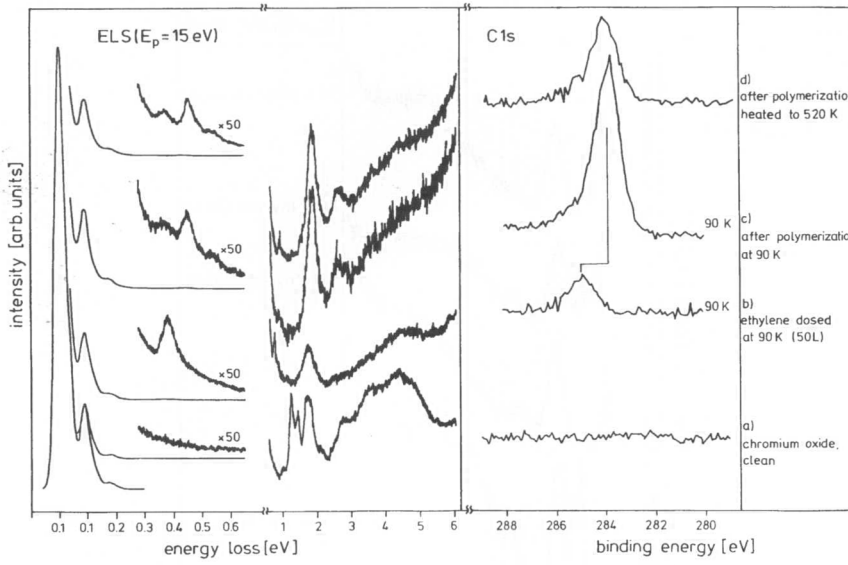


**Fig. 7.** XPS (C1s) and ELS spectra of clean $Cr_2O_3$(0001) as well as after exposure to ethene at ultrahigh vacuum conditions and 1 bar.

had been removed, carbon (about 50% of the value at low temperature) remains on the surface. Its chemical shift can be clearly distinguished from pure ethene (Fig. 7) and is typical for polyethylene [33–35].

Also, the vibrational spectra are compatible with polyethylene formation as shown on the left hand side of Fig. 7 and in Fig. 8. In the HREEL-spectra the monomer adsorbate gives a very broad band in the C–H stretching range. The width is probably caused by the overlap of symmetric and asymmetric vibrations which cannot be resolved in the present experiment. However the signal to noise ratio is very poor which is caused by the disordered surface topography after polymerization. Nevertheless, the downward shift of the C–H stretching vibrations is in agreement with the results on microcrystalline chromiumoxide. Scarano *et al.* [5] identify an average shift of 124.5 $cm^{-1}$ or 15 meV towards lower frequences after polymerization as compared with the monomer.

The electron energy loss spectra in the electronic regime of the monomer adsorbate are compared with the polymer in Fig. 7. The comparison of those data below 1 eV excitation energy now clearly allows for an identification of the peak at 0.7 eV in the ethene adsorbate, alluded to above: Upon polymerization the CH-vibration is reduced in intensity, and a low intense peak at 450 meV is formed. This is also noticeable in the HREELS data at 5 eV primary electron energy (Fig. 8). In the data taken with 15 eV primary electron energy, but poorer energy resolution (Fig. 7), again the polymer

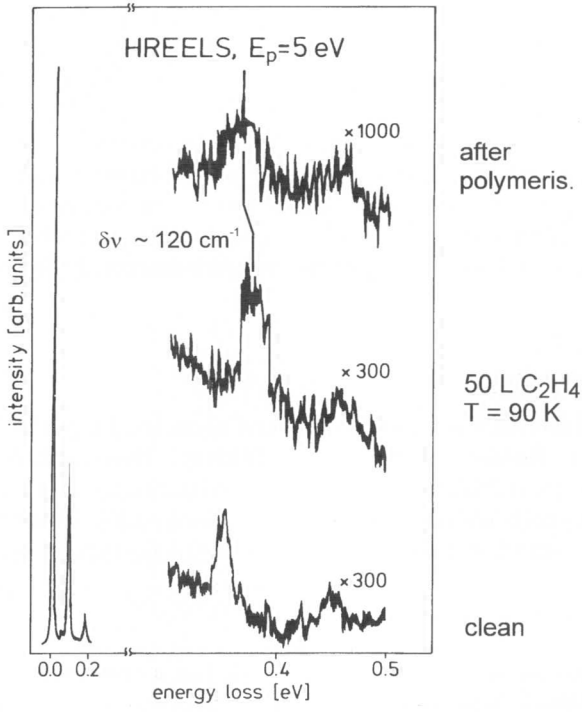


**Fig. 8.** Vibrational spectra of the clean and polymer covered $Cr_2O_3$(0001) surface.

peak is visible, but with lower intensity, while the 450 meV peak is rather pronounced. The latter is compatible with our experience that OH loss intensities increase for higher primary energies [36]. Concomitantly the 0.7 eV double loss is attenuated and a peak shifted to 0.9 eV, shows up. The latter is interpreted as the OH double loss. It is therefore very likely that the 0.7 eV feature is not due to an electronic excitation, although a final assignment is not possible at present. Therefore we assign the peaks at 0.9 eV to the formation of OH on the surface either in the polymerization process [37] or from adsorption of $H_2O$ from the background [13, 36]. We note, however, that OH formation from $H_2O$ adsorption on the clean surface is widely suppressed [36]. We cannot exclude, of course, that the polymer covered surface influences the formation of OH from adsorbed water.

## 4. Summary

We have shown via a combination of various techniques (XPS, TDS, IRAS, HREELS and ELS) that ethene chemisorbs on $Cr_2O_3$(0001) via interaction

with the metal ions on the surface inducing a small charge transfer from the molecule towards the surface. After the chemisorbed layer is saturated ethene may physisorb on the surface in addition. Predosing the surface with oxygen leads to a strong attenuation of the ethene adsorption. Under ultrahigh vacuum conditions adsorption is fully reversible. If, however, the surface is treated with ethene slightly above room temperature under atmospheric pressures then a polymer is formed on the surface whose XPS and ELS characteristics in the vibrational and electronic regime are compatible with the formation of polyethene and simultaneously hydroxyl groups on the surface.

## Acknowledgements

Our research has been supported by several agencies: Deutsche Forschungsgemeinschaft, Bundesministerium für Bildung, Wissenschaft, Forschung und Technologie (BMBF), Ministerium für Wissenschaft und Forschung des Landes Nordrhein-Westfalen, European Communities (Brite-Euram) and Fonds der chemischen Industrie. We are grateful for their support.

## References

1. H. L. Krauss and H. Stach, Inorg. Nucl. Chem. Lett. **4** (1968) 393.
2. M. P. McDaniel, Adv. Catal. **33** (1985) 47.
3. G. Ghiotti, E. Garrone and A. Zecchina, J. Mol. Catal. **65** (1991) 73.
4. A. Zecchina, G. Spoto, G. Ghiotti and E. Garrone, J. Mol. Catal. **86** (1994) 432.
5. D. Scarano, G. Spoto, S. Bordiga, L. Carnelli, G. Ricchiardi and A. Zecchina, Langmuir **10** (1994) 3094.
6. B. Rebenstorf, J. Polymer Sci. A **29** (1991) 1949.
7. G. Spoto, S. Bordiga, E. Garrone, G. Ghiotti and A. Zecchina, J. Mol. Catal. **74** (1992) 175.
8. C. Xu, B. Dillmann, H. Kuhlenbeck and H.-J. Freund, Phys. Rev. Lett. **67** (1991) 3551.
9. H. Kuhlenbeck, C. Xu, B. Dillmann, M. Haßel, B. Adam, D. Ehrlich, S. Wohlrab, H.-J. Freund, U. A. Ditzinger, H. Neddermeyer, M. Neuber and M. Neumann, Ber. Bunsenges. Phys. Chem. **96** (1992) 15.
10. M. Haßel, Diploma Thesis, Ruhr-Universität Bochum (1991).
11. C. Xu, PhD Thesis, Ruhr-Universität Bochum (1991).
12. M. Bender, D. Ehrlich, I. N. Yakovkin, F. Rohr, M. Bäumer, H. Kuhlenbeck, H.-J. Freund and V. Staemmler, J. Phys. Cond. Mat. **7** (1995) 5289.
13. D. Ehrlich, PhD Thesis, Ruhr-Universität Bochum (1995).
14. M. Bender, I. N. Yakovkin and H.-J. Freund, Surf. Sci., submitted.
15. M. E. Grayson and M. P. McDaniel, J. Mol. Catal. **65** (1991) 139.
16. M. P. McDaniel and S. J. Martin, J. Phys. Chem. **95** (1991) 3289.
17. D. D. Beck and J. H. Lunsford, J. Catal. **68** (1981) 121; D. L. Myers and J. H. Lunsford, J. Catal. **92** (1985) 260; J. Catal. **99** (1986) 140.
18. I. E. Wachs, Catal. Today, in press.
19. DuSoung Kim and I. E. Wachs, J. Catal. **142** (1993) 166; M. A. Vuurman, E. D. Hardcastle and I. E. Wachs; J. Mol. Catal. **84** (1993) 193; M. A. Vuurman, I. E. Wachs, D. J. Hufkens and A. Oskam, J. Mol. Catal. **80** (1993) 209.

20. H.-J. Freund, B. Dillmann, O. Seiferth, G. Klivenyi, M. Bender, D. Ehrlich, I. Hemmerich and D. Cappus, Catal. Today, in press.
21. I. Hemmerich, Dissertation, Ruhr-Universität Bochum (1995), unpublished.
22. B. Dillmann, PhD Thesis, Ruhr-Universität Bochum, in preparation.
23. F. Rohr, PhD Thesis, Ruhr-Universität Bochum, in preparation.
24. B. Dillmann, O. Seiferth, M. Bäumer, G. Klivenyi, F. Rohr and H.-J. Freund, to be published.
25. J. Weidlein, V. Müller and K. Dehnicke, *Schwingungsspektroskopie. Eine Einführung*, p. 98, Georg Thieme Verlag, Stuttgart, New York (1982).
26. H. A. Pearce and N. Sheppard, Surf. Sci. **59** (1976) 205.
27. R. E. Kirby, E. L. Garwin, F. K. King and A. R. Nyaiesh, J. Appl. Phys. **62** (1987) 1400.
28. L. Brillson, Surf. Sci. Rep. **2** (1982) 123.
29. W. Mönch, *Semiconductor Surfaces and Interfaces*, Springer Series in Surface Science, Vol. 26, Springer Verlag, Heidelberg (1993).
30. C. R. Brundle, Surf. Sci. **48** (1975) 99.
31. T. E. Felter, W. H. Weinberg, P. A. Zhdan and G. K. Boreskov, Surf. Sci. Lett. **97** (1980) 313.
32. J. L. Solomon, R. J. Madix and J. Stöhr, Surf. Sci. **255** (1991) 30.
33. R. Merryfield, M. P. McDaniel and G. Parks, J. Catal. **77** (1982) 348.
34. F. Maury and F. Ossola, Thin Solid Films **219** (1992) 24.
35. J. J. Pireaux, Ch. Gregoire, R. Caudano, M. Rei Vilar, R. Brinkhuis and A. J. Schouten, Langmuir **7** (1991) 2433.
36. D. Cappus, C. Xu, D. Ehrlich, B. Dillmann, C. A. Ventrice Jr., K. Al-Shamery, H. Kuhlenbeck and H.-J. Freund, Chem. Phys. **177** (1983) 533.
37. M. Nishijima, T. Sekitani, J. Yoshinobu and M. Onchi, Surf. Sci. **242** (1991) 493.